Published in final edited form as:
Pigment Cell Melanoma Res. 2013 March ; 26(2): 247–258. doi:10.1111/pcmr.12063.

Endothelin-1 is a transcriptional target of p53 in epidermal keratinocytes and regulates UV induced melanocyte homeostasis

Stephen Hyter[1,2], **Daniel J. Coleman**[1,2], **Gitali Ganguli-Indra**[1,2], **Gary F. Merrill**[3,4], **Steven Ma**[6], **Masashi Yanagisawa**[7], and **Arup K. Indra**[1,2,3,5]

[1]Department of Pharmaceutical Sciences, Oregon State University, Corvallis, Oregon, USA

[2]Molecular and Cellular Biology Program, Oregon State University, Corvallis, Oregon, USA

[3]Environmental Health Science Center, Oregon State University, Corvallis, Oregon, USA

[4]Department of Biochemistry and Biophysics, Oregon State University, Corvallis, Oregon, USA

[5]Department of Dermatology, Oregon Health and Science University, Portland, Oregon, USA

[6]Immunology Core Laboratory, National Institute of Allergy and Infectious Diseases, Bethesda, Maryland, USA

[7]Department of Molecular Genetics, University of Texas Southwestern Medical Center at Dallas, Dallas, Texas, USA

Summary

Keratinocytes contribute to melanocyte activity by influencing their microenvironment, in part, through secretion of paracrine factors. Here we discovered that p53 directly regulates *Edn1* expression in epidermal keratinocytes and controls UV-induced melanocyte homeostasis. Selective ablation of EDN1 in murine epidermis (EDN1$^{ep-/-}$) does not alter melanocyte homeostasis in newborn skin but decreases dermal melanocytes in adult skin. Results showed that keratinocytic EDN1 in a non-cell autonomous manner controls melanocyte proliferation, migration, DNA damage and apoptosis after UVB irradiation. Expression of other keratinocyte derived paracrine factors did not compensate for the loss of EDN1. Topical treatment with EDN1 receptor (EDNRB) antagonist BQ788 abrogated UV induced melanocyte activation and recapitulated the phenotype seen in EDN1$^{ep-/-}$ mice. Altogether, present studies establish an essential role of EDN1 in epidermal keratinocytes to mediate UV induced melanocyte homeostasis *in vivo*.

Keywords

EDN1; p53; paracrine; UVB; BQ788

Introduction

Endothelin 1 (EDN1) belongs to a group of related peptides (EDN1, EDN2 and EDN3) encoded by separate genes. The mature 21-amino acid peptides are expressed in a variety of

CORRESPONDANCE, Tel: 541-737-5775 (AI); Fax: 541-737-3999 (AI), arup.indra@oregonstate.edu.

Conflict of interest
The authors declare that no conflicting interests exist.

tissue types and activate two distinct G protein-coupled receptors (EDNRA and EDNRB) with varying affinities (Yanagisawa et al., 1988; Arai et al., 1990; Sakurai et al., 1990). The EDNRB receptor is required for melanocyte development from a neural crest lineage (Reid et al., 1996; Opdecamp et al., 1998). Mice deficient in EDN1 have respiratory complications as well as craniofacial abnormalities (Kurihara et al., 1994), while those lacking EDNRB have a spotted color resulting from loss of epidermal melanocytes (Hosoda et al., 1994). Although EDN1 was initially characterized as a potent vasoconstrictive peptide, it also functions as a keratinocyte-derived paracrine factor for melanocytes. Previous *in vitro* studies have shown that ultraviolet B (UVB) exposure increases secretion of keratinocyte-derived EDN1 which regulates proliferation, melanogenesis, migration and dendricity of human melanocytes via a receptor-mediated pathway (Imokawa et al., 1992; Imokawa et al., 1995; Hara et al., 1995; Horikawa et al., 1995), and this stimulatory effect is dampened by the EDNRB antagonist BQ788 (Wu et al., 2004). There was also evidence that EDNRB serves as a tumor progression marker of human melanoma, as increased expression of EDNRB was found in human melanoma biopsies and usage of EDNRB antagonists inhibited melanoma growth (Demunter et al., 2001; Lahav et al., 1999). Additionally, EDN1 was shown to be upregulated in the epidermis of mice after UVB irradiation (Ahn et al., 1998), potentially contributing to the photoprotective effects of EDN1 on melanocytes (Kadekaro et al., 2005). The melanocytic response to UV exposure in mouse skin has been characterized, where follicular melanocytes migrate upward along the outer root sheath and populate the basal layer of the interfollicular epidermis. This epidermal melanocyte population peaks around 72hrs post-UV and begins to decrease 1-2 days later (Rosdahl and Szabo, 1978; Walker et al., 2009). Melanin pigmentation is a result of reciprocal interaction between epidermal keratinocytes and follicular melanocytes through production of various signaling molecules and activation of corresponding receptors on the target cells (Slominski et al., 2004; Slominski et al., 2005b). However, the full spectrum of keratinocytic influence on melanocyte activity after UV exposure remains to be determined.

Our previous work in an $RXR\alpha^{ep-/-}/CDK4^{R24C/R24C}$ cutaneous melanoma model suggested a paracrine contribution by several keratinocyte-derived soluble factors including EDN1 in disease progression (Hyter et al., 2010). Here we discovered a direct *in vivo* transcriptional regulation of keratinocytic *Edn1* by the tumor-suppressor p53 in epidermal keratinocytes in response to UV irradiation. We also demonstrate that *in vivo* disruption of keratinocyte-derived EDN1 signaling *in vivo* alters melanocyte proliferation and decreases epidermal and dermal melanocyte populations in both normal and UV exposed mouse skin. EDN1 also has a protective role against UVR induced DNA damage and apoptosis. Similar effects on UV-induced melanocyte proliferation and DNA damage are observed in p53-null mice. Inhibition of EDN1 signaling by topical application of an EDNRB antagonist BQ788 on mouse skin has similar effects as epidermal EDN1 ablation. Furthermore, treatment of primary murine melanocytes with BQ788 abrogates signaling downstream of this receptor. These findings further support the role of a micro-environmental influence driven by p53 in keratinocytes on the behavior and activation of melanocytes.

Results

Transcriptional regulator p53 directly and positively regulates *Edn1* expression in epidermal keratinocytes after UV irradiation

We wanted to elucidate mechanism(s) of *Edn1* regulation in keratinocytes in response to UV radiation. Induction of p53 after UV exposure protects epidermal keratinocytes against DNA damage skin carcinogenesis (Jiang et al., 1999), and directly regulates *p21* expression to limit cell proliferation. Similar regulation of *Pomc* by p53 in epidermal keratinocytes has been postulated to mediate UV-induced hyperpigmentation in murine skin (Cui et al., 2007). However, this linear mode of action does not fully explain the eumelanogenesis

demonstrated by the melanogenic phenotype of POMC-null mice (Slominski et al., 2005a). To determine if p53 is an upstream regulator of *Edn1* gene in epidermal murine keratinocytes, we performed *in silico* promoter analysis using the fuzznuc and ConTra programs. Three potential p53 consensus binding motifs were identified in proximal, mid and distal promoter region of *Edn1* within 5kb upstream of the transcriptional start site (Figure 1A). Additional *in silico* studies were performed on the human *EDN1* promoter and potential p53 binding sequences were also discovered (Figure 1A). To determine if p53 is recruited onto the promoter of murine *Edn1*, we performed *ex vivo* chromatin immunoprecipitation (ChIP) assay on extracts from primary keratinocytes exposed to UV irradiation using primers designed to capture the three regions, as well as the 3' UTR region. *p21*, a p53 target in keratinocytes, was used as a positive control (Liu and Pelling, 1995). As reported earlier, amplification of isolated chromatin DNA revealed increased promoter occupancy by p53 on the *p21* promoter following UV irradiation (UVR) (Figure S1C). The distal promoter region (relative to the transcriptional start site) of *Edn1* displayed a preferential increase in p53 binding post-UVR compared to other regions and to mock irradiated cells (Figure 1B). These results suggest a possible direct regulation of *Edn1* expression by p53 in epidermal keratinocytes. In order to validate these findings, we performed RT-qPCR analyses for *Edn1* expression in the epidermis of both wildtype (WT) and p53-null ($p53^{-/-}$) adult mice after UVR exposure. A significant decrease in the expression of *Edn1* was observed in the epidermis of $p53^{-/-}$ mice 8hrs post-UVR compared to wildtype skin (Figure 1C). Altogether, these results establish *Edn1* as a direct transcriptional target of p53 in murine keratinocytes.

Keratinocyte specific ablation of EDN1 alters melanocyte homeostasis in the skin of adult mice

The *in vivo* role of keratinocyte-derived EDN1 in regulating epidermal homeostasis and melanocyte activity is unknown. In the present study, we investigated the role of this signaling molecule on keratinocyte and melanocyte homeostasis in murine skin. To this end, floxed $EDN1^{L2/L2}$ mice (Huang et al., 2002; Shohet et al., 2004) were bred with a K14-Cre deleter mouse strain, which drives expression of Cre-recombinase in the basal cells of developing epidermis, thereby generating $EDN1^{ep-/-}$ mice (selectively lacking EDN1 in murine epidermis). Deletion of *Edn1* in presence of Cre was confirmed by PCR using specific primers on DNA isolated from neonatal $EDN1^{L2/L2}$ (control, CT) and $EDN1^{ep-/-}$ mice skin (Figure 2A). RT-qPCR analyses on RNA isolated from the epidermis of CT and $EDN1^{ep-/-}$ mice showed a significant downregulation of *Edn1* transcripts in the mutant skin, confirming ablation of *Edn1* in epidermal keratinocytes (Figure 2B). Basal levels of EDN1 mRNA seen in the $EDN1^{ep-/-}$ skin are most likely due to less frequent *Edn1* expressing cells within the dermal compartment. No compensatory upregulation of *Edn3* (another endothelin family member expressed in skin) transcripts was observed by RT-qPCR in $EDN1^{ep-/-}$ skin compared to CT skin (Figure 2B). Gross morphological examination did not reveal any difference between the skin of $EDN1^{L2/L2}$ and $EDN1^{ep-/-}$ mice.

To determine whether loss of keratinocytic EDN1 altered keratinocyte proliferation and differentiation *in vivo*, we performed histological and immunohistochemical (IHC) analysis on dorsal skin sections from CT and mutant neonatal (P2) and adult (P42) mice. Histological analyses on H&E stained skin sections from CT and mutant mice did not reveal any differences in epidermal thickness between the two groups in the neonatal or adult skin (Figure S2A, B and S6A, B, C). Furthermore, expression pattern for markers of proliferation [Ki67, PCNA, keratin-14 (K14)] and differentiation [K10 and loricrin] were similar between CT and $EDN1^{ep-/-}$ P2 and P42 skin (Figure S2C, D and S6C and data not shown). These results indicate that loss of keratinocytic EDN1 is dispensable for normal epidermal homeostasis of the developing and adult murine epidermis. Fontana-Masson (FM) and TRP1

(melanocyte specific marker) IHC staining on adult skin sections showed a significant decrease in the number of dermal melanocytes in the mutant compared to CT skin. Melanocytes were rarely detected in the CT and mutant adult epidermis. However, no differences in melanocyte number were observed between the neonatal CT and mutant skin (Figure 2C, D and E). Altogether, these findings suggest that EDN1 mediated paracrine signaling from keratinocytes is necessary for maintenance of dermal melanocyte populations in unirradiated adult murine skin.

Role of keratinocytic EDN1 in regulating UV induced proliferation, DNA damage repair and apoptosis of melanocytes *in vivo*

UV irradiation induces secretion of EDN1 by epidermal keratinocytes (Imokawa et al., 1992). In order to investigate the effects of UV irradiation in absence of EDN1, we subjected neonatal $EDN1^{L2/L2}$ and $EDN1^{ep-/-}$ mice to UVR exposure and analyzed its responses on skin keratinocytes and melanocytes. Briefly, P2 pups were exposed to a single dose of $600mJ/cm^2$ UVR and dorsal skin samples were collected after 24, 48, 72 and 96hrs post-treatment. As reported earlier, *Edn1* transcript level was significantly increased in the epidermis of CT skin at 24hrs post-UVR (Ahn et al., 1998) (Figure 3A). No *Edn1* induction was observed in the mutant skin, further confirming Cre-mediated excision of *Edn1* gene in their epidermis (Figure 3A). Although *Edn1* expression decreased in the CT skin after 24hrs post-UVR, its transcript level remained significantly higher at later timepoints compared to the $EDN1^{ep-/-}$ skin. RT-qPCR analyses did not reveal any compensatory upregulation of *Edn3* transcript levels or alteration in the expression level of other keratinocyte derived soluble factors, such as *Fgf2, Hgf, Pomc* or *Kitlg*, in the $EDN1^{ep-/-}$ neonatal mice skin at all timepoints post-UV irradiation (Figure 3A and Figure S3A). These results suggest that any effects on melanocyte activity after UV exposure observed in the present study are solely due to the loss of EDN1. H&E staining on paraffin skin sections from CT and mutant mice did not reveal any differences in epidermal thickness between the CT and mutant skin post-UVR, implying that the loss of keratinocytic EDN1 did not influence UV-induced epidermal hyperplasia (Figure S6A and S6B). To further evaluate any altered responses to UVR, we performed FM staining for pigmented melanocytes on skin sections from CT and mutant mice at different timepoints after UV exposure. We did not observe an increase in epidermal melanocyte population until 72hrs post-UVR in both the groups, and the number of epidermal and dermal melanocytes was significantly reduced in the $EDN1^{ep-/-}$ skin compared to CT skin at 72 and 96hrs post-UVR (Figure 3B, C and D).

In an attempt to elucidate the mechanistic basis of reduced melanocyte population from the hair follicles in the $EDN1^{ep-/-}$ skin, IHC analyses was performed on CT and mutant skin to investigate the proliferative potential, DNA damage and apoptotic responses of melanocytes post-UVR. Co-immunostaining of paraffin skin sections with proliferation markers PCNA or Ki67 with TRP1 allowed us to quantify the proliferative responses to UV exposure in epidermis, dermis and melanocytes. A significant decrease in the number of proliferating melanocytes was seen in the mutant skin after 72hrs UVR using both the proliferation markers, which correlated with the decreased numbers of total melanocytes at that timepoint (Figure 4A and B and S5A and B, left panels). Similarly, IHC analyses for UVR induced DNA damage, using co-labeled anti-CPD and anti-TRP1 antibodies, showed a significant decrease in clearance of thymine dimers in melanocytes from $EDN1^{ep-/-}$ skin at the same timepoint (Figure 4A and B, middle panel). Analyses of melanocyte apoptosis by a modified TUNEL-IHC assay revealed a modest increase in apoptotic melanocytes at 24hrs post-UV irradiation in the $EDN1^{ep-/-}$ skin compared to CT (Figure 4A and B, right panel). We did not observe any difference in the rate of proliferation, DNA damage or apoptosis in epidermal keratinocytes of the CT and mutant skin post-UVR (Figure S6C). Similarly, the dermal proliferation was comparable between CT and MT skin post-UVR at all timepoints.

However, we observed a decrease in DNA damage and apoptosis in the dermis after 72 and 24hrs post-UVR, respectively (Figure S6D). Altogether, our *in vivo* results suggest that keratinocytic EDN1 alone is an important determinant of melanocyte homeostasis and plays a significant role in the proliferation and photoprotection of melanocytes after UV irradiation in neonatal mice.

In order to determine if the non-cell autonomous role of keratinocytic EDN1 is mediated through EDNRB receptor on melanocytes, selective EDNRB antagonist BQ788 was applied to the dorsal skin of wildtype C57BL/6 neonatal mice concurrent with UVR exposure (Ishikawa et al., 1994; Lahav et al., 1999). A significant decrease in the number of epidermal melanocytes was observed by FM staining, and by IHC for TRP1+ cells, 72hrs post-UVR in the BQ788 treated group compared to the vehicle treatment (Figure 3E). We did not notice effects on the dermal melanocyte population, possibly due to an inadequate penetration of BQ788 through the skin barrier (Figure S4C). No significant difference in the percentage of $TRP1^{+}/PCNA^{+}$ proliferating melanocytes was observed by IHC analyses between the two groups (BQ788 vs vehicle) of mice (Figure S4C). Altogether, results demonstrated that *in vivo* blocking of EDNRB activity recapitulates the impaired paracrine effects on melanocytes observed in $EDN1^{ep-/-}$ mice. Present results further support the *in vivo* contribution of EDN1/EDNRB signaling pathway to UVR induced melanocyte activation, migration and proliferation, and demonstrates the feasibility of topical treatments for manipulating melanocyte activation in skin.

Phenotypic similarities of the melanocytic response post-UV exposure between $EDN1^{ep-/-}$ and $p53^{-/-}$ mice

The ability of p53 to bind and regulate melanogenic factors in mice has been previously reported. In order to corroborate our findings for transcriptional regulation of murine *Edn1* by p53, we utilized p53-null ($p53^{-/-}$) mice to evaluate the melanocytic response after UV-exposure. FM staining and IHC utilizing antibodies against TRP1 showed a dramatic decrease in the number of melanocytes that populate the murine epidermis 72hrs after UV exposure (Figure 5A). That was further verified by quantifying both the FM-positive and TRP1-positive cells to ensure that only those from the melanocytic lineage are counted (Figure 5B). Furthermore, IHC analyses for UV-induced DNA damage and melanocyte proliferation using anti-CPD and anti-PCNA or anti-Ki67 antibodies confirmed a significant increase in DNA damageretaining melanocytes and a decrease in proliferating melanocytes in the p53-null skin (Figure 5C and S5A and B). Similar results were obtained after UVR in the $EDN1^{ep-/-}$ mice skin at that time point. Altogether, our results support an important role of p53, upregulated following UV exposure, to bind multiple factors and assist in the regulation of paracrine melanogenic networks.

EDN1 mediates activation of MAPK and PKC signaling through its receptor EDNRB in murine melanocytes

Previous studies in human melanocytes have highlighted the contributions of both MAPK and PKC activation by EDN1 signaling (Imokawa et al., 1996; Sato-Jin et al., 2008; Imokawa et al., 2000). To verify expression of EDNRB receptor in keratinocytes and mature murine melanocytes, we performed immunoblots for EDNRB on lysates prepared from primary keratinocytes and melanocytes (Figure 6A). We hypothesized that lack of activation of MAPK and PKC pathways downstream of EDNRB in melanocytes contribute to their impaired activation and proliferation in $EDN1^{ep-/-}$ mice. To test that, we investigated the effects of exogenous EDN1 on activation of those pathways in murine melanocytes. Briefly, PKC and MAPK activation was analyzed in primary murine melanocytes cultured in complete or minimal medium supplemented with EDN1 and in presence of EDNRB antagonist BQ788. Western blot analyses on cell extracts from melanocytes conditioned

with complete or minimal medium supplemented with EDN1 indicated strong phosphorylation of p42/p44 (pERK) proteins compared to those exposed to minimal media (Figure 6B). Parallel treatment with BQ788 completely abrogated ERK1/2 phosphorylation, indicating EDNRB receptor mediated activation of MAPK in presence of EDN1 (Figure 6B). Furthermore, PKC activity was measured to confirm activation of this pathway downstream of EDNRB. Treatment of minimal medium with EDN1 induced PKC activation in a time-dependent manner, and the kinase activity was completely abolished upon treatment with BQ788, confirming the role of EDNRB receptor for this signaling (Figure 6C). Altogether, above results confirm EDNRB receptor mediated activation of downstream MAPK and PKC pathways in murine melanocytes in presence of exogenous EDN1, and establishes a parallel between mouse and human melanocytes.

It is possible that the loss of keratinocytic EDN1 in our $EDN1^{ep-/-}$ model leads to decreased follicular melanocytes migrating along the upper root sheath, resulting in a lower population of epidermal melanocytes post-UV exposure. We therefore investigated the effects of exogenous EDN1 on the migration of wild type melanocytes using an *in vitro* real-time transwell migration assay. Results indicated that EDN1 is sufficient to increase the rate of transwell migration of cultured melanocytes compared to minimal media alone, supporting the role of keratinocytic EDN1 as a melanocyte chemoattractant (Figure 6D).

In order to determine the *in vivo* physiological effects of EDN1 signaling on melanocytes we further performed IHC for pERK on $EDN1^{L2/L2}$ and $EDN1^{ep-/-}$ neonatal mouse skin after UV exposure. Strikingly, there was a strong induction of pERK 24hrs after UV exposure in the control and mutant epidermis (Figure 6E). That upregulation decreases at 48hrs and reverted to basal levels by 72hrs post-UVR (Figure 6E and F). Importantly, a similar induction of pERK was seen in follicular melanocytes as well, although that induction was modestly reduced in the skin of $EDN1^{ep-/-}$ mice 24hrs post-UVR (Figure 6G). These results verify the *in vivo* activation of MAPK pathway in murine melanocytes post-UV exposure.

Discussion

EDN1 contributes to human melanogenesis and is upregulated in keratinocytes exposed to UVR. In the present study we discovered *Edn1* is a transcriptional target of p53 in epidermal keratinocytes and established an essential role of EDN1 in regulating melanocyte homeostasis and UVR induced photoprotection. Our previous work demonstrated a positive regulation of *Edn1* by RXRα in murine keratinocytes (Hyter et al., 2010). That led us to investigate the mechanisms of regulation of this paracrine factor after exposure to the solar carcinogen UVR. Our RT-qPCR data on p53 null epidermis, together with the ChIP assay for p53 recruitment on the distal region of *Edn1* gene promoter in murine keratinocytes post-UVR, have established p53 as a positive transcriptional regulator of *Edn1* gene in UVR exposed mouse skin. Recently, multiple studies have investigated the role of p53 transcriptional regulation on pigmentation and *in silico* analyses have confirmed presence of p53 binding motifs on promoters of melanogenic factors *KITLG* and *FGF2* (Wei et al., 2006). Concerning p53 regulated UVR induction of *Pomc* (precursor to α–MSH) (Cui et al., 2007), we were able to show a recruitment of p53 on the *Pomc* promoter in murine keratinocytes (Figure S1A). However, under our experimental conditions *Pomc* transcript levels were unaltered in the epidermis of $p53^{-/-}$ mice before and after UV irradiation (Figure S1B). This is consistent with unaltered melanin pigmentation observed after *Pomc* deletion on the same genetic background (Slominski et al., 2005a), suggesting EDN1 signaling could provide alternate mechanisms of eumelanogenesis within the skin. Of note, melanocytes are known to upregulate expression of *MC1R* in response to EDN1 (Tada et al., 1998). Elevated expression of *p53* together with *KITLG, EDN1* and *POMC* has been

previously reported in the epidermis of hyperpigmented human skin, further suggesting a possible role of p53 in activating pigmentation networks (Murase et al., 2009). Also, ChIP combined with a yeast-based assay led to the identification of p53 binding sites on the promoter of *EDN2*, an EDN1 family member, in human mammary epithelial cells (Hearnes et al., 2005). The phenotypic similarities of the melanocytic response observed between $EDN1^{ep-/-}$ and $p53^{-/-}$ mice post- UV exposure underscores the role of keratinocytic p53 to regulate expression of multiple paracrine factors (e.g. EDN1) and mediate melanocyte homeostasis.

The loss of dermal melanocyte populations observed in unirradiated $EDN1^{ep-/-}$ adult mice further emphasizes the existence of paracrine relationship between keratinocytes and melanocytes and underscores the existence of distinct signaling pathways in modulating epidermal vs. dermal melanocytes (Aoki et al., 2009). As this discrepancy in dermal melanocytes is only present in adult and not neonatal mice, it suggests a temporal aspect of EDN1-EDNRB signaling during post-developmental homeostasis and emphasizes EDN1 function in maintenance of adult melanocyte homeostasis. Although epidermal melanocytes are absent in adult mouse skin compared to humans, resident dermal melanocytes are present (Fitzpatrick and Shiseidō, 1981). It is believed that epidermal melanocytes and dermal melanocytes represent distinct populations of cells exhibiting different sensitivities to signaling factors (Aoki et al., 2009; Slominski et al., 2005b). Reliance of dermal melanocytes on EDN1/EDNRB signaling could partly account for the decrease in the number of viable dermal melanocytes in our $EDN1^{ep-/-}$ mice model and establishes a non-cell autonomous role of keratinocytic EDN1 in melanocyte homeostasis. However, no alterations of epidermal proliferation and/or differentiation were seen in the skin of $EDN1^{ep-/-}$ mice due to the loss of keratinocytic EDN1, suggesting that EDN1 is dispensable for controlling epidermal homeostasis. That was in agreement with an earlier report showing no increase in proliferation of cultured human keratinocytes in response to exogenous EDN1 (Yohn et al., 1994).

Our results demonstrate that the overall decrease in the melanocyte population in absence of keratinocytic EDN1 observed 72 and 96hrs post-UVR could be, at least in part, due to decreased melanocyte proliferation around that timepoint. The significant and paradoxical decrease of melanocyte proliferation 72hrs after UVR indicates a role of EDN1 signaling in regulating melanocyte proliferation at the point when melanocytes are activated and migrating out of the hair follicles to repopulate the interfollicular epidermis (Walker et al., 2009). By 96hrs post-UVR, the percentage of proliferating melanocytes is similar between CT and mutant skin, suggesting melanocytes that are able to colonize the epidermal tissue in EDN1−/− skin will eventually respond to alternative keratinocyte-derived paracrine factors. However, total numbers of melanocytes were still reduced in $EDN1^{ep-/-}$ skin at this later timepoint, indicating a possible EDN1-EDNRB contribution towards migration and survival. In addition, the decrease in CPD clearance along with increased apoptosis and altered melanocyte migration could be other potential mechanisms contributing to the overall decrease in melanocyte population in the mutant skin post-UVR. Previous studies utilizing cultured human melanocytes have demonstrated the contribution of EDN1 supplementation in enhancing melanocytic proliferation (Yada et al., 1991). Our present *in vivo* observation of decreased melanocyte proliferation in absence of keratinocytic EDN1, but in the presence of other diffusible paracrine factors (KITLG, HGF, FGF2 and α-MSH), further corroborates those *in vitro* studies. The synergistic induction of multiple UV-induced paracrine factors such as EDN1, FGF2 and POMC-derived peptides makes it difficult to elucidate individual contributions in an *in vivo* model (Swope et al., 1995; Tada et al., 1998). Detecting EDNRB expression on primary murine melanocytes, along with a reduced number of proliferating epidermal melanocytes noted in our $EDN1^{ep-/-}$ skin post-UVR, suggests a role for EDN1/EDNRB signaling in melanocyte activation. It has been previously shown that exogenous

EDN1 can protect cultured human melanocytes from UVRinduced apoptosis, while at the same time enhancing repair of CPD formations in those cells (Kadekaro et al., 2005). The reduced clearance of UVR induced thymine dimers and the modest increase in melanocyte apoptosis observed post-UVR in our EDN1$^{ep-/-}$ mice further validates the previous *in vitro* findings. Our results suggest that cells of the melanocytic lineage have impaired CPD repair capacity in absence of EDN1 signaling compared to other cell types of the skin, thereby predisposing them towards neoplastic transformation. Similar phenotypes in p53$^{-/-}$ mice further support the importance of p53 signaling to the UVR melanocytic response. Additional studies are required to determine which paracrine factors, besides *Edn1* and *Pomc*, are upregulated by p53 in keratinocytes after UV exposure.

Our present results demonstrate that selective inhibition of EDN1 receptor (EDNRB) in cultured murine melanocytes abrogated downstream signaling by inhibiting PKC activation and MAPK pathway, corroborating previous results in human melanocytes (Imokawa et al., 1996; Imokawa et al., 2000; Sato-Jin et al., 2008). The activation of MAPK and PKC by EDN1 in cultured human melanocytes is synergistically enhanced with the addition of KITLG (Imokawa et al., 2000), supporting the role of multiple keratinocyte-derived signaling factors working in tandem to initiate melanocytic activity. Our *in vivo* IHC data for ERK activation suggest that loss of keratinocytic EDN1 did not significantly abolish pERK induction in melanocytes, possibly due to the presence of additional keratinocytic-derived paracrine mitogenic factors in the cellular millieu. Due to the increasing reliance on mouse melanoma models for translational therapeutic approaches in humans, it is important to verify that comparable transduction mechanisms exist downstream of the EDNRB receptor in murine melanocytes. Our data of reduced epidermal melanocyte population after topical treatment with EDNRB receptor antagonist supports our *in vivo* observation where expression of several UVR induced paracrine factors such as KITLG, α–MSH, HGF and FGF2 could not compensate for the loss of EDN1 in the murine epidermis. The modulation of MITF-M has been linked to EDN1 stimulation (Sato-Jin et al., 2008), thereby connecting growth factor receptor signaling to the master regulator of melanocytes. It has also been previously shown that contribution of EDN1 to migration of human melanocytes is superior to FGF2, KITLG and a α–MSH analog (Horikawa et al., 1995; Scott et al., 1997). Our studies of melanocyte migration in presence or absence of EDN1 suggests a possible *in vivo* role of keratinocytic EDN1 in stimulating follicular melanocyte migration to the murine epidermis post-UVR.

Our present findings shed light on the complex interplay between keratinocytes and melanocytes in skin in response to UV irradiation and provide evidence for the possibility of therapeutic manipulation of those pathways. We discovered that p53 regulated secretion of diffusible factors such as EDN1 from epidermal keratinocytes can initiate signaling cascades within melanocytes and control melanocyte homeostasis in response to solar UV-irradiation. What is not currently understood is how these factors act in combination to establish the full spectrum of receptor-mediated cellular responses. Additional studies are necessary to further elucidate the temporal events that occur post-UV exposure within the skin. Understanding how paracrine factors act as photoprotectors against DNA damage and prevent malignant transformation of melanocytes in the cellular microenvironment is crucial for improved treatment of UV-induced skin cancers.

Methods

Mice

Generation of EDN1$^{L2/L2}$ mice has been previously described (Huang et al, 2002). To selectively ablate EDN1 in epidermal keratinocytes, mice carrying LoxP-site-containing (floxed) *Edn1* alleles were bred with hemizygous K14-Cre transgenic mice (Li et al., 2001)

backcrossed to a C57BL/6 background in order to generate $EDN1^{ep-/-}$ mice in mendelian ratios. A semiquantitative PCR was performed in an Eppendorf thermal cycler using primers to amplify the *Cre*, L2 and L- *Edn1* alleles. Mice were housed in our approved University Animal Facility with 12h light cycles, food and water were provided ad libitum, and institutional approval was granted for all animal experiments.

UVR treatment

P2 $EDN1^{L2/L2}$ and $EDN1^{ep-/-}$ mice were exposed to a single dose of 600mJ/cm^2 of UVB light from a bank of four Philips FS-40 UV sunlamps. The irradiance of the sunlamps was measured with an IL-1400A radiometer with an SEE240 UVB detector (International Light). Mice were euthanized 24, 48, 72 and 96hrs after UVR and skin samples retrieved. 0hr samples were taken from P2 mice not exposed to UVR. Cohorts of 5 to 8 age-matched mice from multiple litters were utilized per time point. C57BL/6 $p53^{-/-}$ adult mice were exposed to 600mJ/cm^2 of UVB followed by biopsies taken at 8, 24 and 72hrs post-UVR, while C57BL/6 $p53^{-/-}$ neonatal mice were treated with the same dosage at P3.

BQ788 topical application

BQ788 (A.G. Scientific) was dissolved in ethanol to a 200μM working solution and 20μl was applied to the dorsal skin of P1 C57BL/6 mice once a day for seven treatments. 600mJ/cm^2 UVB exposure was administered on day P3 and skin samples were collected 72 and 96hr post-UVR. Ethanol application alone was used for vehicle control samples.

Histological analyses

Skin biopsies were fixed and stained with hematoxylin and eosin (H&E) as previously described (Indra et al., 2007). Fontana-Masson staining was performed according to manufactures instructions (American MasterTech). All microscopic studies were performed using a Leica DME light microscope and analyzed using the Leica Application Suite software, version 3.3.1.

Immunohistochemistry

Immunofluorescence studies were performed as previously described (Hyter et al, 2010). The following antibodies were used for immunohistochemistry: anti-PEP1 (kindly provided by V. Hearing, NIH, 1:1000), anti-PCNA (Abcam, ab29, 1:6000), anti-CPD (Kamiya Biomedical Company, MC-062, 1:200), anti-pERK (Abcam, ab50011, 1:200), anti-Ki67 (Novocastra, NCL-Ki67-MM1, 1:200) and anti-EDN1 (Peninsula Laboratories, T-4050, 1:1000). The secondary antibodies used were goat anti-rabbit CY2 (1:400) and goat anti-mouse CY3 (1:1000) (Jackson ImmunoResearch). For dual TUNEL-IHC staining, the DeadEnd™ TUNEL System (Promega) was combined with the above protocol. Sections stained without primary antibody was used as a negative control, and all experiments were performed in triplicates. All images were captured using a Zeiss AXIO Imager.Z1 with a digital AxioCam HRm and processed using AxioVision 4.7 and Photoshop. Data were analyzed using ImageJ software (NIH), multiple IHC fields on each slide from all groups were randomly chosen and 10–15 fields per slide were counted. The slides were analyzed independently in a double-blinded manner by two investigators and significance was determined using a Student's t-test.

Reverse transcription–quantitative PCR (RT-qPCR) analyses

Total RNA was extracted from whole dorsal skin or epidermal tail skin using Trizol (Invitrogen) and cDNA was created using SuperScript III RT (Invitrogen). Amplification was performed on an ABI Real Time PCR machine using a QuantiTect SYBR Green PCR kit (Invitrogen), and all targets were normalized to the internal control *Hprt*. All reactions

were performed in triplicates using a minimum of three biological replicates from each group of mice. Melting curve analyses were performed to ensure specificity of amplification. Statistical analysis was done with GraphPad Prism software.

Immunoblotting analyses

Primary C57BL/6 murine melanocytes were obtained from the Yale University Cell Culture Core. Cells were maintained in a complete melanocyte growth medium consisting of F-12 nutrient mixture (Ham), 8% FBS, bovine pituitary extract (25μg/mL), TPA (10ng/mL), 3-isobutyl-1-methylxanthine (22μg/mL) and 1X antibiotic/antimycotic. Melanocytes were starved into a quiescent state using a minimal culture medium containing F-12 nutrient mixture (Ham), 8% FBS and 1X antibiotic/antimycotic for 72hrs prior to experiment. Cells were pre-incubated with the EDNRB antagonist BQ788 (A.G. Scientific) or vehicle in minimal culture medium for 60 minutes prior to treatment, followed by addition of EDN1 (Sigma). All treatments were prepared in minimal culture medium and cells exposed to minimal medium alone or complete melanocyte growth medium were used as negative and positive controls, respectively. At the appropriate time points, protein lysates were obtained by collecting cells in a lysis buffer (20mM HEPES, 250mM NaCl, 2mM EDTA, 1% SDS, 10% glycerol, 50mM NaF, .1mM hemin chloride, 5mM NEM, 1mM PMSF and 10μg/mL leupeptin and aproptinin) followed by sonication. Protein concentration was performed using the BCA assay (Thermo Scientific). Equal amounts of protein extract (15μg) from each lysate were resolved using sodium dodecyl sulfate polyacrylamide gel electrophoresis and transferred onto a nitrocellulose membrane. The blots were blocked overnight with 5% nonfat dry milk and incubated with specific antibodies. The antibodies used were rabbit anti-endothelin receptor B (#AER-002, Alomone labs), total ERK (#4695, Cell Signaling) and phospho-ERK (#9101, Cell Signaling). After incubation with the appropriate secondary antibody, signals were detected using immunochemiluminescent reagents (GE Healthcare, Piscataway, NJ). Equal protein loading in each lane was confirmed with a β-actin antibody (#A300-491, Bethyl).

PKC kinase activity assay

Murine melanocytes were grown and treated as described above. Cells were lysated at the designated timepoints using cold lysis buffer (20mM MOPS, 50mM β-glycerolphosphate, 50mM sodium fluoride, 1mM sodium vanadate, 2mM EGTA, 2mM EDTA, 1%NP40, 1mM DTT, 1mM benzamidine, 1mM PMSF and 10μg/mL leupeptin and aproptinin). Cold lysates were collected and sonicated to ensure disruption and cytosolic fraction was collected using centrifugation. Protein concentration was determined as described above. Relative kinase activity was measured using the PKC Kinase Activity assay kit (Enzo) according to the manufacturers instructions.

Real-time migration assay

Murine melanocytes were starved into a quiescent state using a minimal culture medium for 48hrs prior to experiment as described above. Cells were seeded into a CIM-plate 16 using an xCELLigence system (Roche) at a density of 2×10^4 according to manufacturer's instructions. All assays were performed in triplicate and data analysis was performed using xCELLigence software.

Chromatin immunoprecipitation

Primary mouse keratinocytes from wild-type B6 pups were exposed without a lid to 10mJ/cm^2 UV irradiation. Fresh media was applied and the cells were allowed to incubate for 2hrs. Chromatin precipitation was performed as previously described (Hyter et al, 2010)

using either 2μg of a p53 antibody (Santa Cruz Biotechnology) or non-specific IgG (Santa Cruz Biotechnology). Experiments were performed a minimum of three times.

RT-qPCR Primers

All RT-qPCR and genotyping primers are available upon request.

Acknowledgments

We would like to thanks Sharmeen Chagani for assistance in the histological analyses. We also thank Drs. Mark Zabriskie and Gary DeLander of the OSU College of Pharmacy for continuous support and encouragement. These studies were supported by grant ES016629-01A1 (AI) from NIEHS at National Institutes of Health, an OHSU Medical Research Foundation grant to AI, and by a NIEHS Center grant (ES00210) to the Oregon State University Environmental Health Sciences Center. The project described was also supported by Award Number T32 ES007060 from the National Institute of Environmental Health Sciences (NIEHS) and by the National Cancer Institute of the National Institutes of Health under award number T32CA106195 "Training in the Molecular Basis of Skin/Mucosa Pathobiology" to OHSU from the National Cancer Institute. The content is solely the responsibility of the authors and does not necessarily represent the official views of NIEHS or the National Institutes of Health (NIH).

References

Ahn GY, Butt KI, Jindo T, Yaguchi H, Tsuboi R, Ogawa H. The expression of endothelin-1 and its binding sites in mouse skin increased after ultraviolet B irradiation or local injection of tumor necrosis factor alpha. J Dermatol. 1998; 25:78–84. [PubMed: 9563273]

Aoki H, Yamada Y, Hara A, Kunisada T. Two distinct types of mouse melanocyte: differential signaling requirement for the maintenance of non-cutaneous and dermal versus epidermal melanocytes. Development. 2009; 136:2511–2521. [PubMed: 19553284]

Arai H, Hori S, Aramori I, Ohkubo H, Nakanishi S. Cloning and expression of a cDNA encoding an endothelin receptor. Nature. 1990; 348:730–732. [PubMed: 2175396]

Cui R, Widlund HR, Feige E, Lin JY, Wilensky DL, Igras VE, D'orazio J, Fung CY, Schanbacher CF, Granter SR, et al. Central role of p53 in the suntan response and pathologic hyperpigmentation. Cell. 2007; 128:853–864. [PubMed: 17350573]

Demunter A, De Wolf-Peeters C, Degreef H, Stas M, Van Den Oord JJ. Expression of the endothelin-B receptor in pigment cell lesions of the skin. Evidence for its role as tumor progression marker in malignant melanoma. Virchows Arch. 2001; 438:485–491. [PubMed: 11407477]

Fitzpatrick, TB.; Shiseidō. Biology and diseases of dermal pigmentation. Tokyo: University of Tokyo Press; 1981. (Tokyo Japan)

Hara M, Yaar M, Gilchrest BA. Endothelin-1 of keratinocyte origin is a mediator of melanocyte dendricity. J Invest Dermatol. 1995; 105:744–748. [PubMed: 7490466]

Hearnes JM, Mays DJ, Schavolt KL, Tang L, Jiang X, Pietenpol JA. Chromatin immunoprecipitation-based screen to identify functional genomic binding sites for sequence-specific transactivators. Molecular and cellular biology. 2005; 25:10148–10158. [PubMed: 16260627]

Horikawa T, Norris DA, Yohn JJ, Zekman T, Travers JB, Morelli JG. Melanocyte mitogens induce both melanocyte chemokinesis and chemotaxis. J Invest Dermatol. 1995; 104:256–259. [PubMed: 7530272]

Hosoda K, Hammer RE, Richardson JA, Baynash AG, Cheung JC, Giaid A, Yanagisawa M. Targeted and natural (piebald-lethal) mutations of endothelin-B receptor gene produce megacolon associated with spotted coat color in mice. Cell. 1994; 79:1267–1276. [PubMed: 8001159]

Huang H, Yanagisawa M, Kisanuki YY, Jelicks LA, Chandra M, Factor SM, Wittner M, Weiss LM, Pestell RG, Shtutin V, et al. Role of cardiac myocyte-derived endothelin-1 in chagasic cardiomyopathy: molecular genetic evidence. Clin Sci (Lond). 2002; 103(Suppl 48):263S–266S. [PubMed: 12193100]

Hyter S, Bajaj G, Liang X, Barbacid M, Ganguli-Indra G, Indra AK. Loss of nuclear receptor RXRalpha in epidermal keratinocytes promotes the formation of CDK4-activated invasive melanomas. Pigment Cell Melanoma Res. 2010; 23:635–648. [PubMed: 20629968]

Imokawa G, Kobayasi T, Miyagishi M. Intracellular signaling mechanisms leading to synergistic effects of endothelin-1 and stem cell factor on proliferation of cultured human melanocytes. Cross-talk via trans-activation of the tyrosine kinase c-kit receptor. J Biol Chem. 2000; 275:33321–33328. [PubMed: 10921922]

Imokawa G, Miyagishi M, Yada Y. Endothelin-1 as a new melanogen: coordinated expression of its gene and the tyrosinase gene in UVB-exposed human epidermis. J Invest Dermatol. 1995; 105:32–37. [PubMed: 7615973]

Imokawa G, Yada Y, Kimura M. Signalling mechanisms of endothelin-induced mitogenesis and melanogenesis in human melanocytes. Biochem J. 1996; 314(Pt 1):305–312. [PubMed: 8660299]

Imokawa G, Yada Y, Miyagishi M. Endothelins secreted from human keratinocytes are intrinsic mitogens for human melanocytes. J Biol Chem. 1992; 267:24675–24680. [PubMed: 1280264]

Indra AK, Castaneda E, Antal MC, Jiang M, Messaddeq N, Meng X, Loehr CV, Gariglio P, Kato S, Wahli W, et al. Malignant transformation of DMBA/TPA-induced papillomas and nevi in the skin of mice selectively lacking retinoid-X-receptor alpha in epidermal keratinocytes. J Invest Dermatol. 2007; 127:1250–1260. [PubMed: 17301838]

Ishikawa K, Ihara M, Noguchi K, Mase T, Mino N, Saeki T, Fukuroda T, Fukami T, Ozaki S, Nagase T, et al. Biochemical and pharmacological profile of a potent and selective endothelin B-receptor antagonist, BQ-788. Proc Natl Acad Sci U S A. 1994; 91:4892–4896. [PubMed: 8197152]

Jiang W, Ananthaswamy HN, Muller HK, Kripke ML. p53 protects against skin cancer induction by UV-B radiation. Oncogene. 1999; 18:4247–4253. [PubMed: 10435637]

Kadekaro AL, Kavanagh R, Kanto H, Terzieva S, Hauser J, Kobayashi N, Schwemberger S, Cornelius J, Babcock G, Shertzer HG, et al. alpha-Melanocortin and endothelin-1 activate antiapoptotic pathways and reduce DNA damage in human melanocytes. Cancer Res. 2005; 65:4292–4299. [PubMed: 15899821]

Kurihara Y, Kurihara H, Suzuki H, Kodama T, Maemura K, Nagai R, Oda H, Kuwaki T, Cao WH, Kamada N, et al. Elevated blood pressure and craniofacial abnormalities in mice deficient in endothelin-1. Nature. 1994; 368:703–710. [PubMed: 8152482]

Lahav R, Heffner G, Patterson PH. An endothelin receptor B antagonist inhibits growth and induces cell death in human melanoma cells in vitro and in vivo. Proc Natl Acad Sci U S A. 1999; 96:11496–11500. [PubMed: 10500205]

Li M, Chiba H, Warot X, Messaddeq N, Gerard C, Chambon P, Metzger D. RXRalpha ablation in skin keratinocytes results in alopecia and epidermal alterations. Development. 2001; 128:675–688. [PubMed: 11171393]

Liu M, Pelling JC. UV-B/A irradiation of mouse keratinocytes results in p53-mediated WAF1/CIP1 expression. Oncogene. 1995; 10:1955–1960. [PubMed: 7761096]

Murase D, Hachiya A, Amano Y, Ohuchi A, Kitahara T, Takema Y. The essential role of p53 in hyperpigmentation of the skin via regulation of paracrine melanogenic cytokine receptor signaling. J Biol Chem. 2009; 284:4343–4353. [PubMed: 19098008]

Opdecamp K, Kos L, Arnheiter H, Pavan WJ. Endothelin signalling in the development of neural crest-derived melanocytes. Biochem Cell Biol. 1998; 76:1093–1099. [PubMed: 10392719]

Reid K, Turnley AM, Maxwell GD, Kurihara Y, Kurihara H, Bartlett PF, Murphy M. Multiple roles for endothelin in melanocyte development: regulation of progenitor number and stimulation of differentiation. Development. 1996; 122:3911–3919. [PubMed: 9012511]

Rosdahl IK, Szabo G. Mitotic activity of epidermal melanocytes in UV-irradiated mouse skin. J Invest Dermatol. 1978; 70:143–148. [PubMed: 632619]

Sakurai T, Yanagisawa M, Takuwa Y, Miyazaki H, Kimura S, Goto K, Masaki T. Cloning of a cDNA encoding a non-isopeptide-selective subtype of the endothelin receptor. Nature. 1990; 348:732–735. [PubMed: 2175397]

Sato-Jin K, Nishimura EK, Akasaka E, Huber W, Nakano H, Miller A, Du J, Wu M, Hanada K, Sawamura D, et al. Epistatic connections between microphthalmia-associated transcription factor and endothelin signaling in Waardenburg syndrome and other pigmentary disorders. FASEB J. 2008; 22:1155–1168. [PubMed: 18039926]

Scott G, Cassidy L, Abdel-Malek Z. Alpha-melanocyte-stimulating hormone and endothelin-1 have opposing effects on melanocyte adhesion, migration, and pp125FAK phosphorylation. Experimental cell research. 1997; 237:19–28. [PubMed: 9417862]

Shohet RV, Kisanuki YY, Zhao XS, Siddiquee Z, Franco F, Yanagisawa M. Mice with cardiomyocyte-specific disruption of the endothelin-1 gene are resistant to hyperthyroid cardiac hypertrophy. Proc Natl Acad Sci U S A. 2004; 101:2088–2093. [PubMed: 14764893]

Slominski A, Plonka PM, Pisarchik A, Smart JL, Tolle V, Wortsman J, Low MJ. Preservation of eumelanin hair pigmentation in proopiomelanocortin-deficient mice on a nonagouti (a/a) genetic background. Endocrinology. 2005a; 146:1245–1253. [PubMed: 15564334]

Slominski A, Tobin DJ, Shibahara S, Wortsman J. Melanin pigmentation in mammalian skin and its hormonal regulation. Physiological reviews. 2004; 84:1155–11228. [PubMed: 15383650]

Slominski A, Wortsman J, Plonka PM, Schallreuter KU, Paus R, Tobin DJ. Hair follicle pigmentation. J Invest Dermatol. 2005b; 124:13–21. [PubMed: 15654948]

Swope VB, Medrano EE, Smalara D, Abdel-Malek ZA. Long-term proliferation of human melanocytes is supported by the physiologic mitogens alpha-melanotropin, endothelin-1, and basic fibroblast growth factor. Experimental cell research. 1995; 217:453–459. [PubMed: 7698246]

Tada A, Suzuki I, Im S, Davis MB, Cornelius J, Babcock G, Nordlund JJ, Abdel-Malek ZA. Endothelin-1 is a paracrine growth factor that modulates melanogenesis of human melanocytes and participates in their responses to ultraviolet radiation. Cell growth & differentiation : the molecular biology journal of the American Association for Cancer Research. 1998; 9:575–584.

Walker GJ, Kimlin MG, Hacker E, Ravishankar S, Muller HK, Beermann F, Hayward NK. Murine neonatal melanocytes exhibit a heightened proliferative response to ultraviolet radiation and migrate to the epidermal basal layer. J Invest Dermatol. 2009; 129:184–193. [PubMed: 18633434]

Wei CL, Wu Q, Vega VB, Chiu KP, Ng P, Zhang T, Shahab A, Yong HC, Fu Y, Weng Z, et al. A global map of p53 transcription-factor binding sites in the human genome. Cell. 2006; 124:207–219. [PubMed: 16413492]

Wu CS, Yu CL, Lan CC, Yu HS. Narrow-band ultraviolet-B stimulates proliferation and migration of cultured melanocytes. Exp Dermatol. 2004; 13:755–763. [PubMed: 15560759]

Yada Y, Higuchi K, Imokawa G. Effects of endothelins on signal transduction and proliferation in human melanocytes. J Biol Chem. 1991; 266:18352–18357. [PubMed: 1917960]

Yanagisawa M, Kurihara H, Kimura S, Tomobe Y, Kobayashi M, Mitsui Y, Yazaki Y, Goto K, Masaki T. A novel potent vasoconstrictor peptide produced by vascular endothelial cells. Nature. 1988; 332:411–415. [PubMed: 2451132]

Yohn JJ, Smith C, Stevens T, Morelli JG, Shurnas LR, Walchak SJ, Hoffman TA, Kelley KK, Escobedo-Morse A, Yanagisawa M, et al. Autoregulation of endothelin-1 secretion by cultured human keratinocytes via the endothelin B receptor. Biochimica et biophysica acta. 1994; 1224:454–458. [PubMed: 7803503]

Significance

Most knowledge of endothelin-1 (EDN1) regulating the proliferation and migration of human melanocytes comes from *in vitro* cell culture studies. Here we investigated the *in vivo* contribution of keratinocytic EDN1 on melanocyte biology. Our data show that keratinocytic *Edn1* is directly regulated by tumor suppressor p53 and is essential to control UV induced melanocyte homeostasis *in vivo*. Results indicate that lack of EDN1 has little effect on melanocyte homeostasis during development, but is necessary for the maintenance of dermal melanocytes in adult skin. Melanocytic proliferation, migration, DNA damage repair and apoptosis can all be modulated through the paracrine mechanism of EDN1. Overall, we present evidence that EDN1 in epidermal keratinocytes regulates melanocyte biology in adulthood and following UV-irradiation *in vivo*.

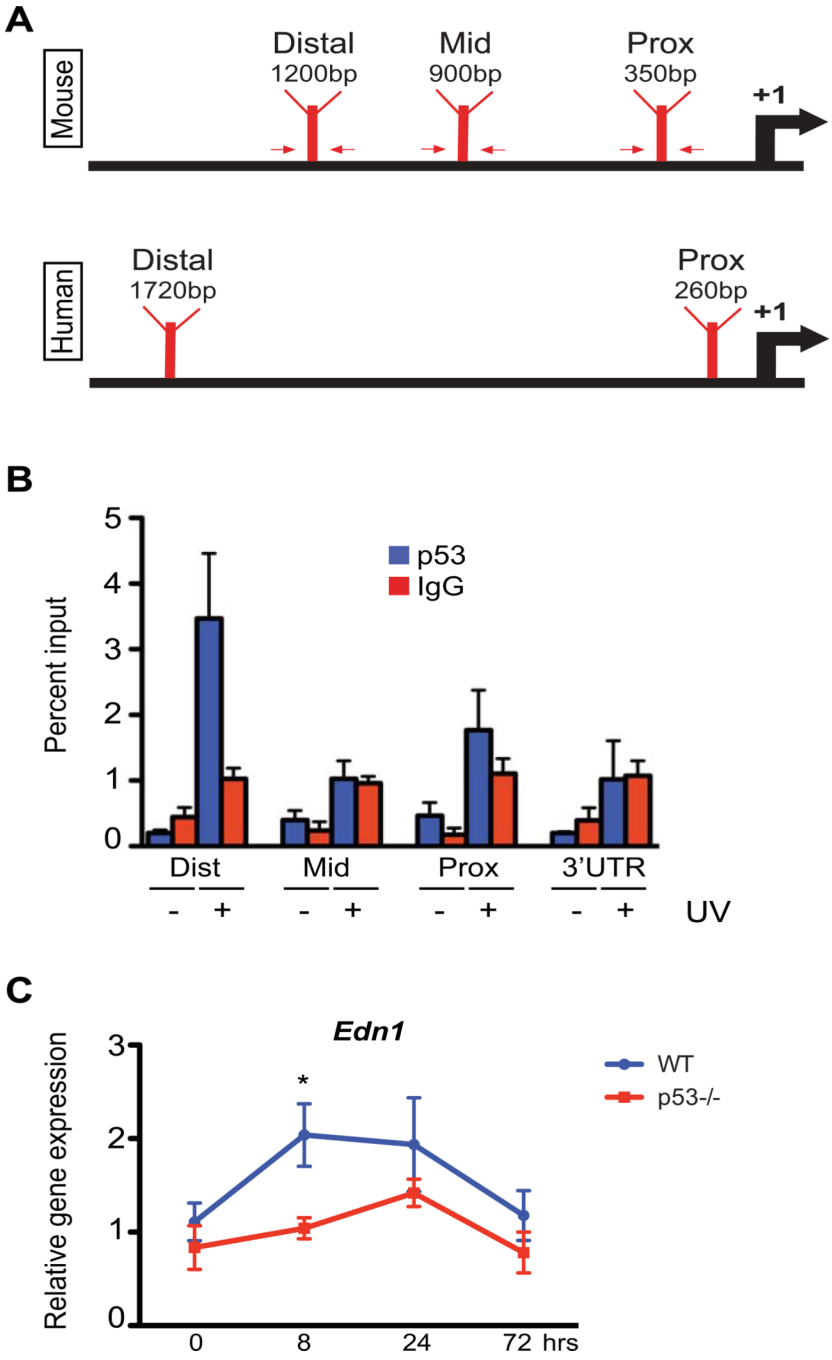

Figure 1.

Positive regulation of *Edn1* expression after UV exposure by p53 in murine keratinocytes. (A) Schematic of predicted p53 binding locations on murine and human *Edn1/EDN1* promoters. Arrows indicate primers designed for chromatin immunoprecipitation (ChIP). (B) ChIP assay on primary murine keratinocytes using anti-p53 antibody following presence or absence of UV exposure. Results were analyzed by qPCR using primers specific to proximal, mid and distal regions (indicated in A). Primers directed against the 3' UTR region of EDN1 and non-specific IgG antibody were used as negative controls. (C) Relative gene expression of *Edn1* in epidermis from adult wildtype C57BL/6 and $p53^{-/-}$ mice at designated time points post-UV exposure. All experiments were done using a minimum of

three biological replicates from each group and in all cases are expressed as mean +/− SEM. Statistical analysis was performed using Graphpad Prism, * = $p < 0.05$.

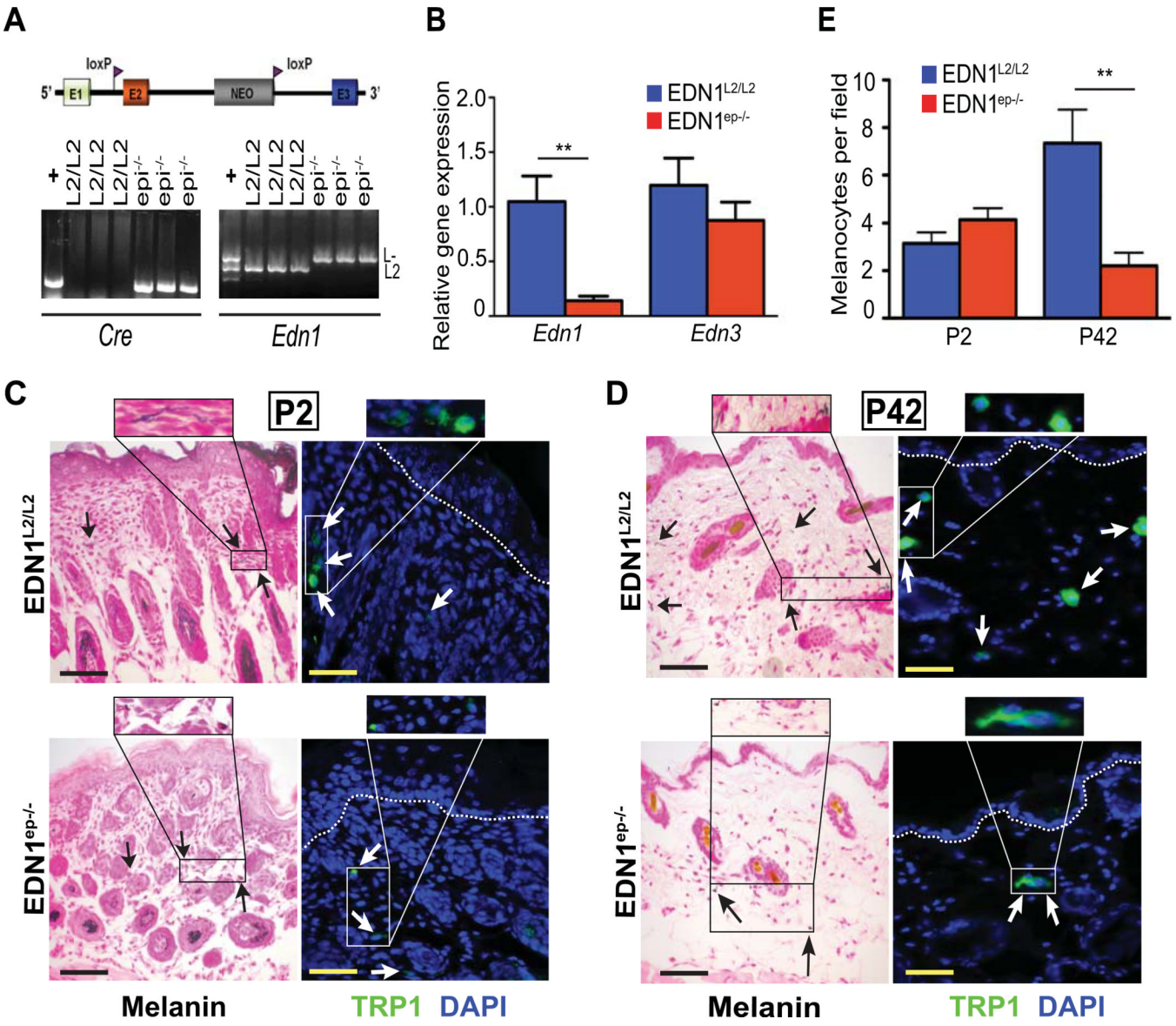

Figure 2.

Characterization of EDN1$^{ep-/-}$ mice showed reduced epidermal and dermal melanocytes in adult skin. (A) Schematic diagram of Cre-targeted loxP sites flanking exon 2 of *Edn1*. Genotyping results using primers directed against both *Cre* and *Edn1* from epidermal genomic DNA. (B) qPCR analysis of mRNA expression levels for *Edn1* and *Edn3* in untreated P2 mouse whole skin are shown. (C,D) Fontana-Masson (black) and TRP1 (green) staining of untreated P2 and P42 mouse dorsal skin sections, arrows indicate dermal melanocytes; scale bar=20μm. IHC sections counterstained with DAPI (blue) and white dashed lines indicate epidermal-dermal junction. (E) Bar graph comparing melanocytes per field between untreated P2 and P42 EDN1$^{L2/L2}$ and EDN1$^{ep-/-}$ skin. All experiments were done using a minimum of three biological replicates from each group and in all cases are expressed as mean +/− SEM. Statistical analysis was performed by Student's t-test using Graphpad Prism, ** = $p < 0.01$.

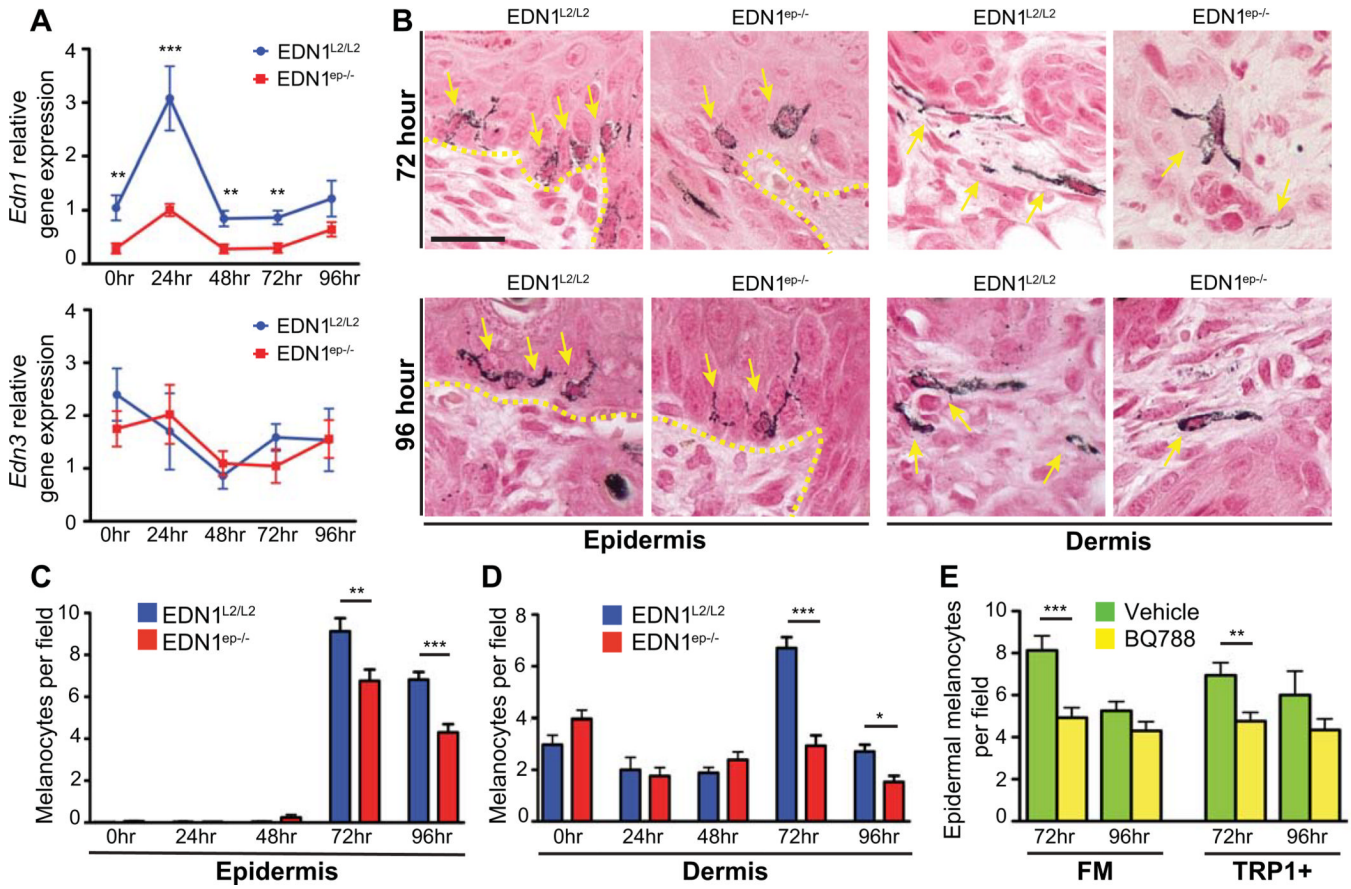

Figure 3.

Decreased epidermal and dermal melanocytes in EDN1$^{ep-/-}$ and BQ788-treated wildtype neonatal skin post-UVR. (A) Relative gene expression of *Edn1* and *Edn3* over time following UVR of EDN1$^{L2/L2}$ and EDN1$^{ep-/-}$ P2 skin. (B) Fontana Masson (FM) stained images at 72 and 96hr post-UVR of P2 skin, arrows indicate melanocytes. Yellow dashed line represents epidermal-dermal junction, scale bar=20μm. (C) Epidermal melanocyte counts per field in EDN1$^{L2/L2}$ and EDN1$^{ep-/-}$ skin over time post- UVR of P2 skin. (D) Dermal melanocyte counts per field in EDN1$^{L2/L2}$ and EDN1$^{ep-/-}$ skin over time post- UVR of P2 skin. (E) Epidermal melanocyte counts per field in wildtype B6 mice treated with topical BQ788 or vehicle at 72 and 96hrs post-UVR of P3 skin for both FM and IHC (TRP1+). All experiments were done using a minimum of three biological replicates from each group of mice and in all cases are expressed as mean +/− SEM. Statistical analysis was performed using Graphpad Prism, * = $p < 0.05$, ** = $p < 0.01$, *** = $p < 0.001$.

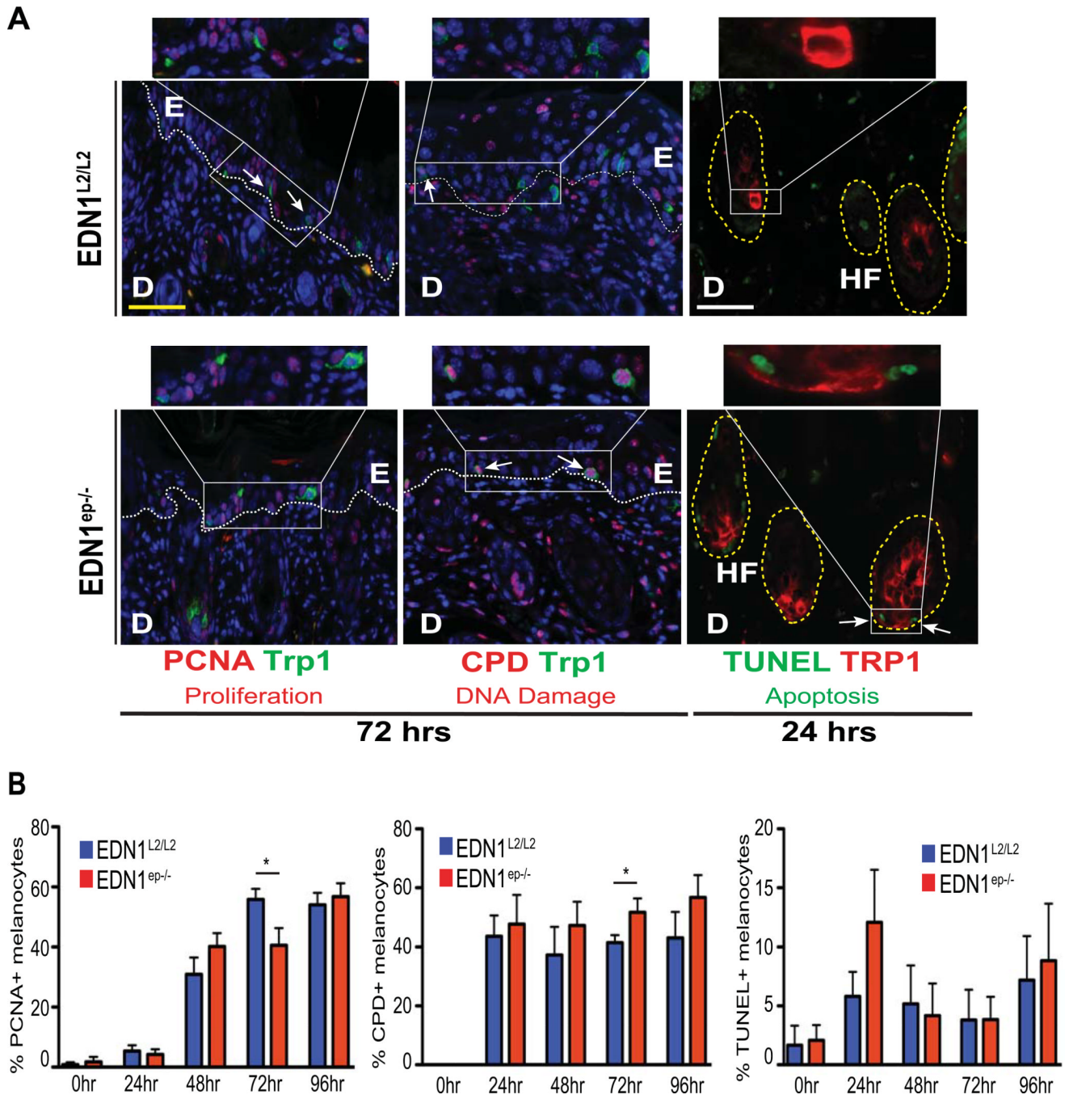

Figure 4.

Immunohistochemical characterization for proliferation, DNA damage and apoptosis of melanocytes post-UVR. (A) IHC analysis of EDN1$^{L2/L2}$ and EDN1$^{ep-/-}$ skin at 72 or 24hrs post-UVR of P2 mice stained with anti-PCNA (red), anti-CPD (red), anti-TRP1 (green and red) primary antibodies and TUNEL assay (green). Yellow scale bar=62μm, white scale bar=20μm. E=epidermis, D=dermis, HF=hair follicle. PCNA and CPD sections counterstained with DAPI (blue) White dashed line indicates dermalepidermal junction. (B) Percentage of PCNA, CPD or TUNEL-positive melanocytes out of total DAPIstained cells between EDN1$^{L2/L2}$ and EDN1$^{ep-/-}$ skin post-UVR of P2 mice. All experiments were done using a minimum of three biological replicates from each group of mice and in all cases are

expressed as mean +/− SEM. Statistical analysis was performed using Graphpad Prism, * = $p < 0.05$.

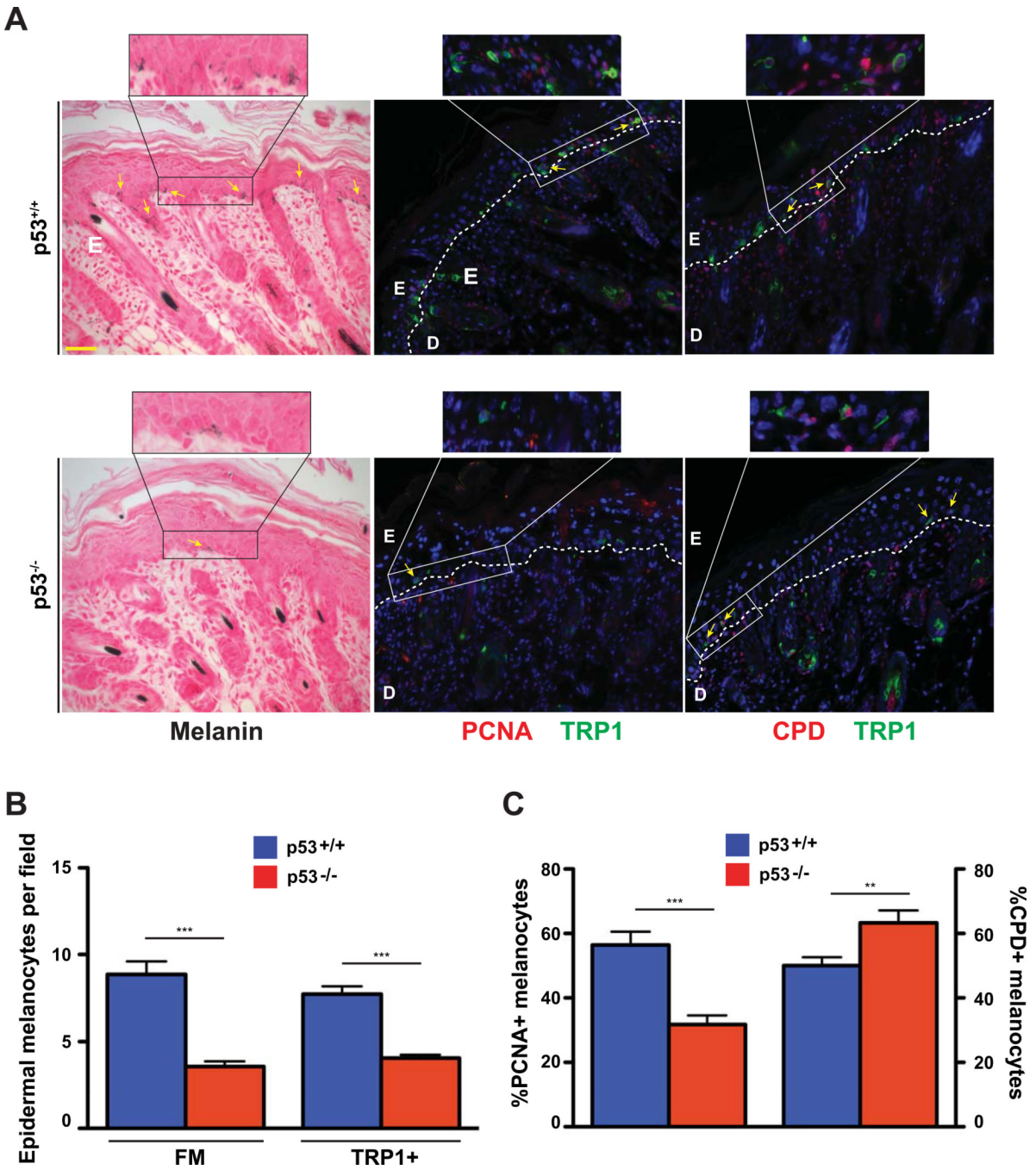

Figure 5.

Decreased epidermal and dermal melanocytes and altered melanocyte proliferation and DNA damage in $p53^{-/-}$ neonatal skin post-UVR. (A) Fontana Masson (FM) and IHC stained images of $p53^{+/+}$ and $p53^{-/-}$ mouse skin at 72hr post-UV treatment of P3 mice, arrows indicate melanocytes. Anti-PCNA (red), anti-CPD (red), anti-TRP1 (green) primary antibodies were used, PCNA and CPD sections counterstained with DAPI (blue). White dashed line represents epidermal-dermal junction, E=epidermis, D=dermis, scale bar=62μm. (B) Epidermal melanocyte counts per field using both FM+ and TRP1+ cells 72 hours post-UVR of P3 skin in $p53^{+/+}$ and $p53^{-/-}$ mice. (C) Percentage of PCNA or CPD positive melanocytes out of total DAPI-stained cells between $p53^{+/+}$ and $p53^{-/-}$ neonatal mice 72

hours post-UVR of P3 mice. All experiments were done using a minimum of three biological replicates from each group of mice and in all cases are expressed as mean +/− SEM. Statistical analysis was performed using Graphpad Prism, ** = $p < 0.01$, *** = $p < 0.001$.

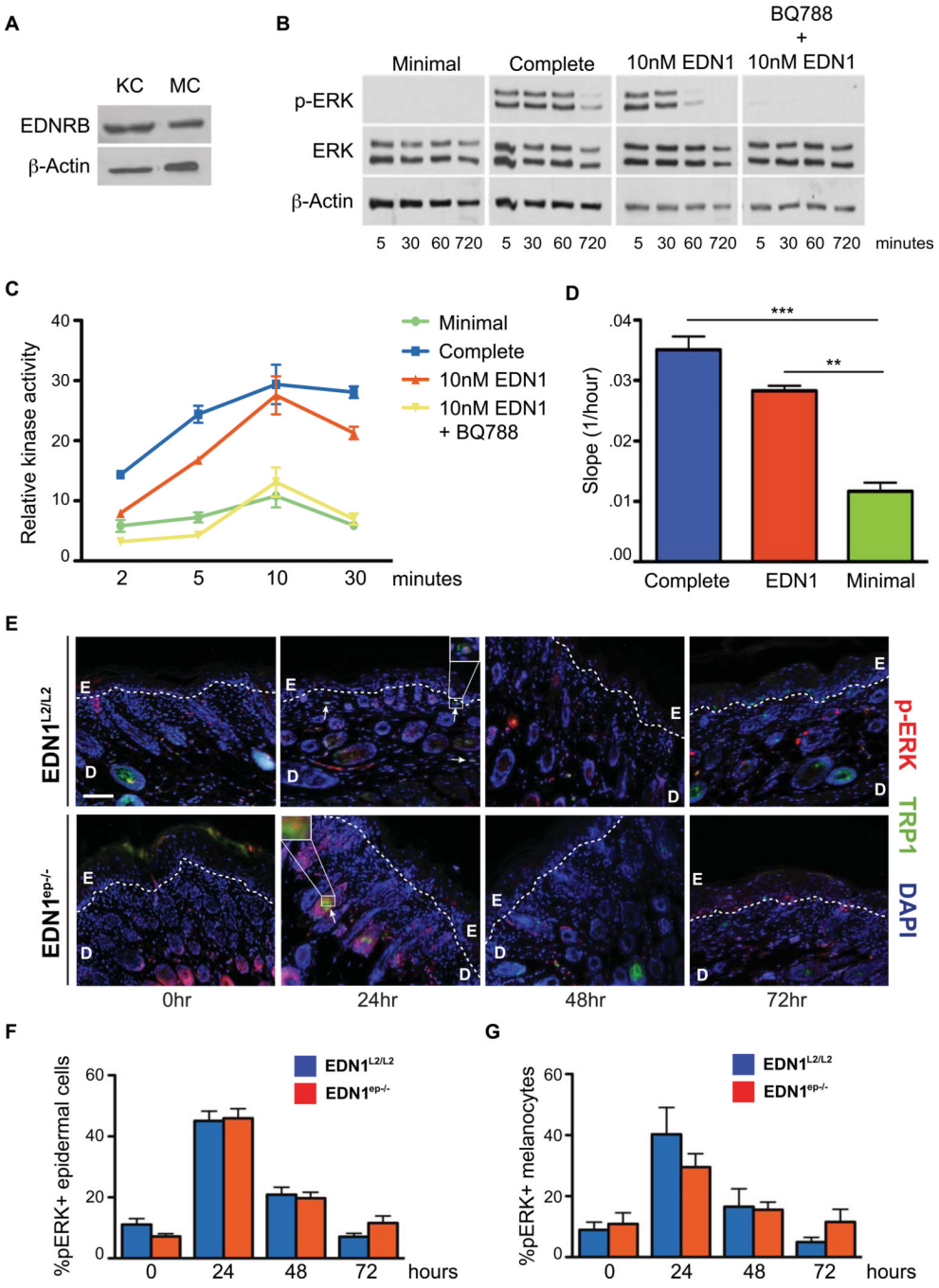

Figure 6.

Activation of MAPK and PKC signaling by EDN1 is specific to EDNRB receptor. (A) Immunoblot analysis of EDNRB expression in lysates from primary murine keratinocytes [KC] and melanocytes [MC], β-actin levels were used as controls. (B) Immunoblot analysis for ERK phosphorylation after addition of exogenous EDN1 with or without the EDNRB antagonist BQ788. Total ERK and β-actin levels were used as controls, as well as minimal and complete mediums. (C) Activation of PKC after addition of exogenous EDN1 with or without the presence of EDNRB antagonist BQ788. All experiments were performed in triplicate and PKC activation results are expressed as mean +/− SEM. (D) Real-time transwell migration assay comparing slopes for exponential migration phase of wildtype

melanocytes. (E) IHC analysis of ERK activation in $EDN1^{L2/L2}$ and $EDN1^{ep-/-}$ skin at 0, 24, 48 and 72hrs post-UVR treatment of P2 mice with anti-pERK (red) and anti-TRP1 (green) primary antibodies. All sections are counterstained with DAPI (blue), white dashed line represents epidermal-dermal junction. E=epidermis, D=dermis, white scale bar=62 μm, arrows and white boxes indicate pERK activated melanocytes. (F) Percentage of pERK+ cells out of total DAPI-stained epidermal cells between $EDN1^{L2/L2}$ and $EDN1^{ep-/-}$ mice post-UVR treatment of P2 mice. (G) Percentage of pERK+ melanocytes out of total TRP1+ stained cells in $EDN1^{L2/L2}$ and $EDN1^{ep-/-}$ after UVR treatment of P2 mice. All experiments were done using a minimum of three biological replicates from each group of mice and in all cases are expressed as mean +/− SEM. Statistical analysis was performed using Graphpad Prism, ** = $p < 0.01$, *** = $p < 0.001$.